2021 43rd Annual International Conference of the
IEEE Engineering in Medicine & Biology Society (EMBC)
Oct 31 - Nov 4, 2021. Virtual Conference

Brain Intrinsic Functional Activity in Relation to Metabolic Changes in Alzheimer's Disease: A Simultaneous PET/fMRI study

Wanqing Sun, Miao Zhang, Yaoyu Zhang, Biao Li, and Yao Li*, *Senior Member, IEEE*

Abstract— **Previous studies have shown that the intrinsic brain functional activity significantly reduced in a variety of regions of Alzheimer's disease (AD) patients. However, the associated underlying metabolic mechanism remains not clear. Brain activity is primarily driven by the dynamic activity of neurons and their interconnections, which are regulated by synapses and are closely related to glucose uptakes. Simultaneous FDG-PET/fMRI imaging provides a unique opportunity to measure the concurrent brain functional activity and cerebral glucose metabolism information. In this study, using simultaneous resting-state PET/fMRI imaging, we investigated the concurrent global intrinsic activity and metabolic signal changes in AD patients. Twenty-two controls and nineteen AD patients were included. We compared the whole-brain amplitude of low frequency fluctuations (ALFF) measured using fMRI imaging and glucose uptake maps acquired from PET imaging between the two groups. Both maps showed significant reductions in the precuneus and left inferior parietal lobule (IPL) in AD compared to the control groups. Moreover, the ALFF within the precuneus and left IPL were significantly correlated with the colocalized glucose metabolism. The ALFF in the left IPL was significantly correlated with patient cognitive performance evaluated using MMSE or MoCA. Our findings provide useful insights into the understanding of brain intrinsic functional-metabolic activity and its role in AD pathology.**

I. Introduction

Alzheimer's Disease (AD) is the most common neurodegenerative disease, but its etiology is not well understood. Using functional magnetic resonance imaging (fMRI), a number of studies have shown alterations of brain functional activities in AD patients compared with cognitively normal older adults [1]. In addition, abnormally reduced intensity of low-frequency fluctuations in the brains of AD patients have been demonstrated [2]. Liang [3] et al. found that amplitude of low frequency fluctuations (ALFF) changed significantly in the early stage of AD, independent of age, sex and atrophy. However, the associated underlying metabolic mechanism remains not clear.

Brain activity is primarily driven by the dynamic activity of neurons and their interconnections, which are regulated by synapses and are closely related to glucose uptakes [4]. In AD patients, distinct patterns of reduced cortical glucose metabolism have been found using ^{18}F-2-fluoro-2-deoxy-D-glucose positron emission tomography (FDG-PET) imaging [5]. Glucose hypometabolism was observed to first occur in the parietal-temporal association area, posterior cingulate cortices, and precuneus, which subsequently spread to the whole cortex with the progression of AD [6]. In specific areas showing hypometabolism in AD patients, the medial frontal gyrus, precuneus and inferior parietal lobule for instance, the FDG-uptakes were closely related to functional activity within the default-mode network (DMN) area [7]. In addition, patients with early-onset AD exhibited more rapid decrease in metabolism in the bilateral parietal and posterior cingulate cortices and precuneus region compared to patients with late-onset AD [8]. Nevertheless, the spatial covariation between brain functional activity and metabolic signal changes in AD has not been fully explored.

Simultaneous FDG-PET/fMRI imaging provides a unique opportunity to measure the concurrent brain functional activity and cerebral glucose metabolism information. It was utilized lately to investigate the coupling of brain functional-metabolic features as well as its relationship to AD pathology. Compared to normal subjects, the bioenergetic coupling between glucose metabolism and the neural information transmission was significantly reduced in AD patients [9]. Therefore, to some extent, the abnormal glucose utilization was associated with the disrupted communication and reduced activity in brain regions susceptible to AD pathology [9].

In this study, using simultaneous resting-state PET/fMRI imaging, we investigated the concurrent global intrinsic activity and metabolic signal changes in AD patients. The spatial covariation features were identified and their relationship to the cognitive performance of AD patients were explored.

II. Methods and Materials

A. Study design

A total of 41 participants were included in the study, including 22 healthy controls (HCs) and 19 AD patients. Demographics of the subjects are listed in Table I. The participants were recruited from the Memory Clinic at Ruijin Hospital, Shanghai. Participants completed the clinical dementia rating (CDR), the Mini-Mental State Examination (MMSE) and Montreal Cognitive Assessment (MoCA) for cognitive function evaluation. Exclusion criteria included: mental illness or other neurological disorders; pregnancy or renal failure; major systemic disease; traumatic brain injury; drugs or alcohol abuse. All participants or their designees provided written informed consents. This study was approved

This research was supported by National Natural Science Foundation of China (No. 81871083); Shanghai Jiao Tong University Scientific and Technological Innovation Funds (2019QYA12); Key Program of Multidisciplinary Cross Research Foundation of Shanghai Jiao Tong University (YG2021ZD28).

Wanqing Sun, Yaoyu Zhang and Yao Li (Tel: +86-21-62932981; e-mail: yaoli@sjtu.edu.cn) are with School of Biomedical Engineering, Shanghai Jiao Tong University, Shanghai, 200030, P.R. China. Miao Zhang and Biao Li are with Department of Nuclear Medicine, Ruijin Hospital, Shanghai Jiao Tong University School of Medicine, Shanghai, 200030, P.R. China.

by the Institutional Review Committee of Ruijin Hospital, according to the ethical standards of the Helsinki declaration.

TABLE I. DEMOGRAPHIC AND NEUROPSYCHOLOGICAL DATA

	HC	AD	p
N	22	19	
Gender (F/M)	10/12	6/13	0.364 [a]
Age, yr	65.64(7.47)	67.26(8.51)	0.814 [b]
Education, yr	13.32(2.42)	11.95(3.21)	0.127 [b]
MMSE	29.55(0.74)	21.37(4.74)	<0.001 [b]
MoCA	28.86(1.12)	16.47(5.74)	<0.001 [b]
CDR	0	⩾0.5	

Values are mean (SD). a. Chi-square test b. One-way ANOVA

Abbreviations: HC: healthy controls; AD: Alzheimer Disease; MMSE: Mini-Mental State Examination; MoCA: Montreal Cognitive Assessment; CDR: Clinical Dementia Rating Scale.

B. Image acquisition

All imaging data were acquired on a Biograph mMR scanner (Siemens Healthcare, Erlangen, Germany). Structural MR images were acquired using T1-weighted magnetization-prepared rapid gradient echo (MPRAGE) sequence (repetition time (TR) = 1900 ms, echo time (TE) = 2.44 ms, field of view (FOV) = 256 mm, voxel size = 0.5 × 0.5 × 1.0 mm^3); resting-state fMRI data were acquired using a gradient-echo echo-planar imaging sequence (TR = 2000 ms, TE = 22 ms, FOV = 192 mm; voxel size = 3 × 3 × 3.75 mm^3). During the scan, the participants were instructed to lay supine with eyes closed but remain awake and avoid systematic thinking. The PET data were acquired at 40 mins after an intravenous bolus injection of ^{18}F-FDG at 3.7 MBq/kg (voxel size = 2.1 × 2.1 × 2.0 mm^3, 127 slices). After corrections of random coincidences, dead-time, scatter and photon attenuation, the PET data were reconstructed using ordered subset expectation maximization (OSEM) algorithm (4 iterations, 21 subsets). Post-filtering was performed using a 2 mm full width half maximum (FWHM) Gaussian filter.

C. FMRI data preprocessing

All the fMRI data preprocessing was carried out using Analysis of Functional Neuroimaging (AFNI, https://afni.nimh.nih.gov) software package [10]. The first four volumes were discarded to avoid noises due to the adaption of subjects to the scanning. Head motion was controlled by nuisance signals regression, and participants with more than 0.5 mm mean framewise displacement were excluded. Nonlinear spatial normalization to MNI space with a resampled resolution of 3 × 3 × 3 mm^3 was applied to all the images. Temporal band-pass filtering with bandwidth of 0.01 - 0.1 Hz was performed to reduce the effect of low-frequency drifts and high-frequency noises. Several nuisance signals, including estimated motion parameters, their first derivatives, as well as the averaged signals from white matter (WM) and cerebral spinal fluid (CSF), were removed using linear regression. Finally, spatial smoothing was carried out for all images with a 6 mm FWHM Gaussian kernel.

D. ALFF analysis

The calculation of ALFF was performed using the Data Processing Assistant for Resting-State fMRI (DPARSF) [11]. The ALFF value has shown important physiological significance in measuring intrinsic or spontaneous neuronal activity in brain regions [12]. For the measurement of ALFF, spatial smoothing was performed beforehand. For a given voxel, the filtered time series was converted to the frequency domain by the fast Fourier transform. The square root of the power spectrum is then calculated and averaged in the range of 0.01 to 0.08 Hz. For a particular voxel, the square root of this average was defined as ALFF. Then, the ALFF was normalized to Z-score of each voxel.

E. PET data preprocessing

The PET image data were preprocessed using SPM12 (https://www.fil.ion.ucl.ac.uk/spm). The PET data of each subject were first registered to the T1-weighted image using affine transformation and then corrected for partial volume effects using the Müller-Gärtner method [13]. The T1-weighted images were spatially normalized to the Montreal Neurological Institute (MNI)-152 template and the transformation parameters were subsequently applied to warp the PET images to the MNI space. After that, the PET data were quantified using the standard uptake value ratio (SUVR) divided by the average uptake in the cerebellar gray matter and spatially smoothed with a 6 mm FWHM Gaussian kernel. Regions with significant differences ($p < 0.01$) in SUVR were extracted for further analysis.

F. Statistical analysis

All the statistical analyses were performed using SPSS software (version 25, IBM Corporation, Armonk, NY, USA). Clinical characteristics were compared between two groups using two-sample t tests. The correlations between ALFF and SUVR as well as the correlations between ALFF and MMSE or MoCA were calculated using Pearson correlation analysis. Age, gender, and education level were used as covariates. A Bonferroni-corrected $p < 0.05$ for multiple comparisons was considered statistically significant.

TABLE II. BRAIN REGIONS WITH SIGNIFICANT DIFFERENCES IN ALFF BETWEEN AD PATIENTS AND HEALTHY CONTROLS

Regions	Cluster Size	T value	MNI (x, y, z)
Parietal_Inf _L	98	-5.0690	-45, -60, 36
Precuneus	101	-4.3578	15, -83, 27
ParaHippocampal_L	124	4.8815	-21, 0, -30

P < 0.01, AlphaSim corrected at cluster level.

III. RESULTS

The demographic characteristics of all participants are listed in Table I. No significant difference was found in age, gender or education level between the HCs and AD groups. The AD patients had significantly lower MMSE or MoCA score ($p < 0.001$) compared to HCs.

Figure 1 shows the differences in whole-brain ALFF and FDG maps between the HC and AD groups. For the AD group, the ALFF values reduced in the left inferior parietal lobule (IPL) and precuneus, and increased in the parahippocampal gyrus, compared to the HC group. Leftward lateralization of ALFF has been shown in IPL. In addition, the SUVR significantly decreased in the inferior parietal lobule, precuneus, temporal lobe and thalamus in AD patients. The details of the clusters with decreased ALFF values were listed in Table II. As can be seen, the regions with concurrent reductions of ALFF and SUVR included the left IPL and precuneus. The between-group comparison for left IPL and

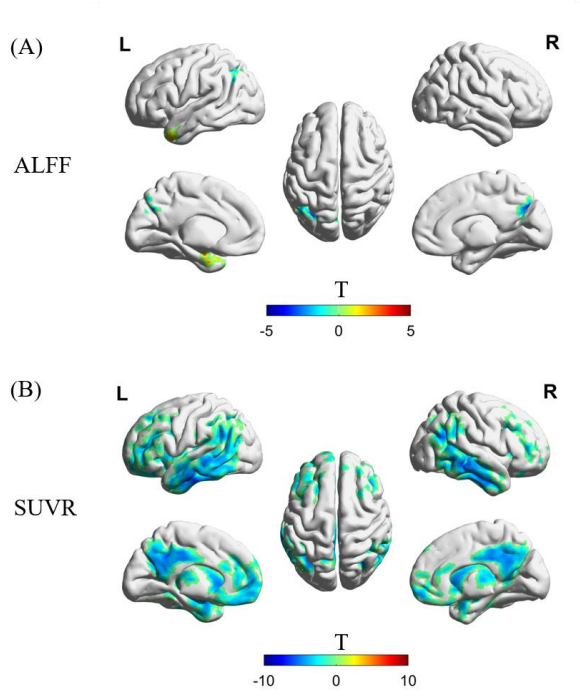

Figure 1. Group differences in ALFF(A) and SUVR(B) between AD patients and healthy controls, respectively.

precuneus of both brain measures were illustrated in Fig. 2. Moreover, there were significant correlations between ALFF and SUVR in both precuneus and left IPL for both groups, which are shown in Figure 3.

In addition, the patient MMSE score was positively correlated with the ALFF of left IPL (p = 0.005, R = 0.662). And the patient MoCA score was positively correlated with the ALFF of left IPL (p = 0.004, R = 0.681) and precuneus (p = 0.008, R = 0.642), respectively, as shown in Fig.4.

IV. Discussion

In this study, we investigated the global brain intrinsic activity and glucose metabolism in the HC and AD groups using simultaneous PET/fMRI imaging. Compared to the HC group, the AD group showed concomitant reductions of functional and metabolic signals in precuneus and inferior parietal lobule.

Both the inferior parietal lobule and precuneus are parts of DMN. Previous functional MRI studies have shown the vulnerability of DMN in AD patients, which might be related to the neurotoxic effects of amyloid beta (Aβ) deposition due to high metabolic stress [14]. Eustache et al. found decreased glucose metabolism in both precuneus and inferior parietal lobule in AD patients [15]. Originated from neurovascular coupling, the fMRI signal is closely related to neuronal activity, and ALFF is closely related to spontaneous neuronal activity. The fMRI signal is co-determined by the cerebral blood flow, cerebral blood volume and cerebral metabolic rate of glucose and oxygen. Therefore, there is a degree of covariation between ALFF measured using fMRI and glucose metabolism measured using PET, in consistence with our findings in Fig.3.

In addition, we observed that the ALFF of left IPL and precuneus were significantly correlated with MMSE or MoCA scores of the AD patients. The ALFF was significantly correlated with SUVR in both precuneus and left IPL. Previous studies have found the aberrant accumulations of amyloid plaques and neurofibrillary tangles in the inferior parietal lobule of mild cognitive impairment (MCI) and AD patients [16.17], which may affect intrinsic neuronal activity. In addition, the reduction of glucose metabolism was consistently found in the parietal lobe of AD patients [15.18]. Studies in primates have demonstrated a link between inferior parietal lobule and the

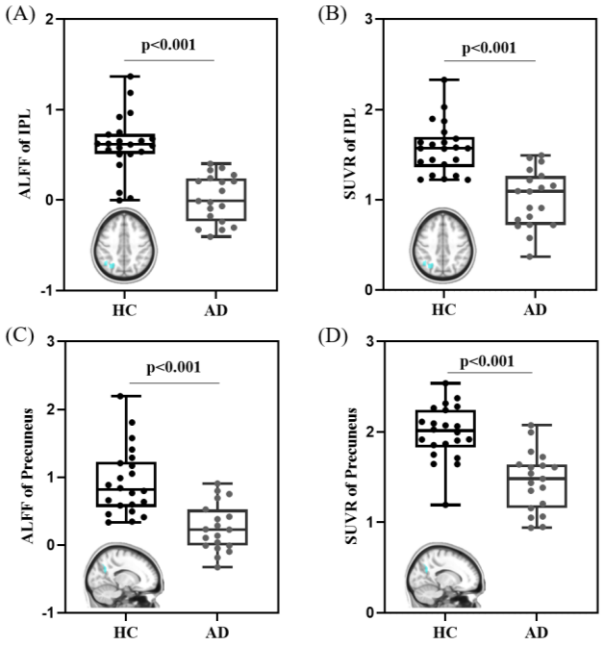

Figure 2. Group differences of ALFF and SUVR in the left IPL and precuneus between AD patients and healthy controls.

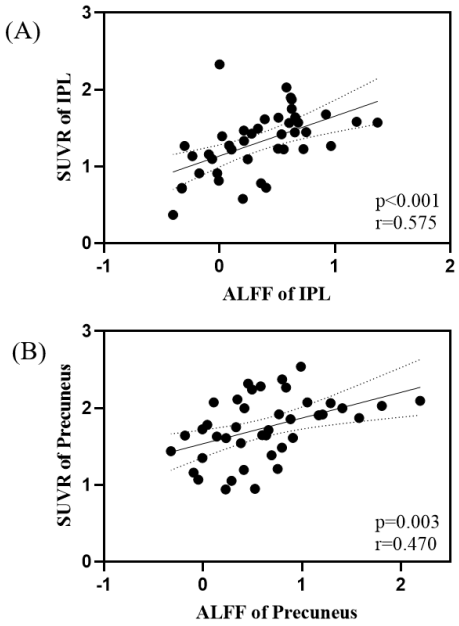

Figure 3. Correlations between ALFF and SUVR in the left IPL and precuneus.

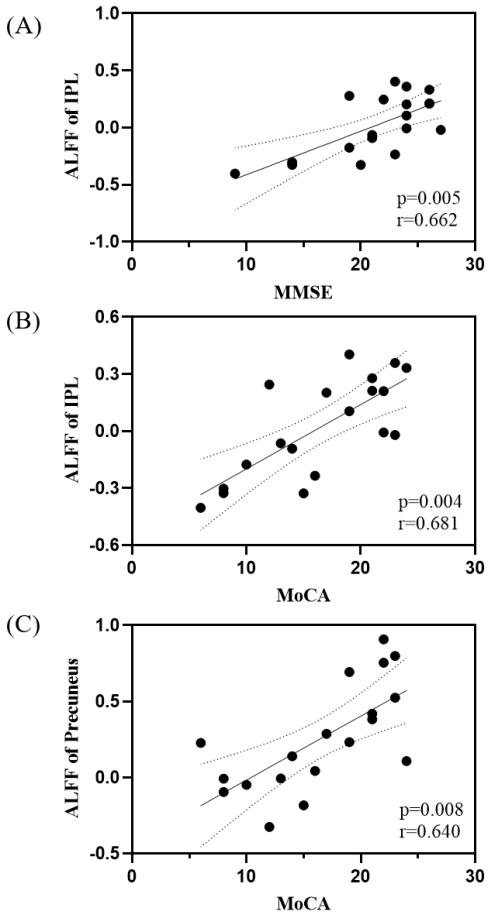

Figure 4. Correlations between ALFF of IPL or precuneus and cognitive scores of AD patients

hippocampus [19], which also suggested that IPL is part of the memory circuit. Furthermore, cognitive functions associated with IPL functions were impaired in early AD, e.g., attention, naming or executive dysfunctions. Our observations went along with previous studies.

The precuneus is an important functional hub of brain network, which is characterized by high metabolism and high oxygen consumption. As a key component of the DMN [20], the precuneus activation has been found during a variety of basic cognitive tasks including episodic memory, visual-spatial imagery, and self-processing [20]. In AD patients, reduced functional activity of precuneus has been consistently found, which was associated with patient cognitive decline [21]. Our findings of precuneus ALFF in association with patients cognitive score are in line with previous findings.

In summary, we investigated the concurrent changes of brain functional and metabolic features globally in AD patients. Decreases in intrinsic activity and glucose metabolism occurred simultaneously in the posterior part of DMN of patients. The positive correlations between ALFF and glucose metabolism in precuneus and IPL indicate a certain degree of coupling between functional activity and metabolism in specific regions. The ALFF in both inferior parietal lobule and precuneus were correlated with cognitive score, suggesting their associations to cognitive impairments of AD patients. Our findings provide useful insights into the understanding of brain intrinsic functional-metabolic activity and its role in AD pathology.

REFERENCES

[1] I. M. McDonough et al. "Risk for Alzheimer's disease: A review of long-term episodic memory encoding and retrieval fMRI studies," Ageing Res Rev, vol. 62, p. 101133, Sep 2020.

[2] X. N. Zuo et al., "The oscillating brain: complex and reliable," Neuroimage, vol. 49, no. 2, pp. 1432-45, Jan 15 2010.

[3] K. Li et al. "Altered amplitude of low-frequency fluctuations in early and late mild cognitive impairment and Alzheimer's disease," Curr Alzheimer Res, vol. 11, no. 4, pp. 389-398, 2014.

[4] A. Drzezga et al., "Neuronal dysfunction and disconnection of cortical hubs in non-demented subjects with elevated amyloid burden," Brain, vol. 134, no. Pt 6, pp. 1635-46, Jun 2011.

[5] R. La Joie et al. "Region-specific hierarchy between atrophy, hypometabolism, and beta-amyloid (Abeta) load in Alzheimer's disease dementia," J Neurosci, vol. 32, no. 46, pp. 16265-73, Nov 14 2012.

[6] S. Minoshima et al."A diagnostic approach in Alzheimer's disease using three-dimensional stereotactic surface projections of fluorine-18-FDG PET," J Nucl Med, vol. 36, no. 7, pp. 1238-48. 1995

[7] S. Passow et al. "Default-mode network functional connectivity is closely related to metabolic activity," Hum Brain Mapp, vol. 36, no. 6, pp. 2027-38, Jun 2015.

[8] E. J. Kim et al. "Glucose metabolism in early onset versus late onset Alzheimer's disease: an SPM analysis of 120 patients," Brain, no. 8, pp. 1790-1801, 2005.

[9] R. Marchitelli et al. "Simultaneous resting-state FDG-PET/fMRI in Alzheimer Disease: Relationship between glucose metabolism and intrinsic activity," Neuroimage, vol. 176, pp. 246-258, Aug 1 2018.

[10] R. W. Cox, "AFNI: Software for Analysis and Visualization of Functional Magnetic Resonance Neuroimages," Comput. Biomed. Res., vol. 29, no. 3, p. 162, 1996.

[11] C. G. Yan et al. "DPABI: Data Processing & Analysis for (Resting-State) Brain Imaging," Neuroinformatics, vol. 14, no. 3, pp. 339-51, Jul 2016.

[12] Y. F. Zang et al. "Altered baseline brain activity in children with ADHD revealed by resting-state functional MRI," Brain Dev, vol. 29, no. 2, pp. 83-91, Mar 2007.

[13] H. W. Muller-Gartner et al. "Measurement of radiotracer concentration in brain gray matter using positron emission tomography: MRI-based correction for partial volume effects," J Cereb Blood Flow Metab, vol. 12, no. 4, pp. 571-583, 1992.

[14] G. Gonzalez-Escamilla et al. "PETPVE12: an SPM toolbox for Partial Volume Effects correction in brain PET - Application to amyloid imaging with AV45-PET," Neuroimage, vol. 147, pp. 669-677, Feb 15 2017.

[15] F. Eustache et al. "'In the course of time': a PET study of the cerebral substrates of autobiographical amnesia in Alzheimer's disease," Brain, vol. 127, no. Pt 7, pp. 1549-60, Jul 2004.

[16] H. Braak and E. Braak, "Neuropathological stageing of Alzheimer-related changes," Acta Neuropathologica, vol. 82, no. 4, pp. 239-259, 1991.

[17] P. T. Nelson et al. "Alzheimer's-type neuropathology in the precuneus is not increased relative to other areas of neocortex across a range of cognitive impairment," Neurosci Lett, vol. 450, no. 3, pp. 336-339, 2009.

[18] M. Lehmann et al. "Diverging patterns of amyloid deposition and hypometabolism in clinical variants of probable Alzheimer's disease," Brain, vol. 136, no. Pt 3, pp. 844-58, Mar 2013.

[19] D. M. Clower et al. "The Inferior Parietal Lobule Is the Target of Output from the Superior Colliculus, Hippocampus, and Cerebellum," J Neurosci, vol. 21, pp. 6283 - 6291, 2001.

[20] A. E. Cavanna and M. R. Trimble, "The precuneus: a review of its functional anatomy and behavioural correlates," Brain, vol. 129, no. Pt 3, pp. 564-83, Mar 2006.

[21] M. E. Raichle et al. "A default mode of brain function,"PNAS, vol. 98, no. 2, pp. 676-682, 2001.